0026-895X/06/7001-60–70$20.00
MOLECULAR PHARMACOLOGY
Copyright © 2006 The American Society for Pharmacology and Experimental Therapeutics
Mol Pharmacol 70:60–70, 2006

Vol. 70, No. 1
21204/3119195
Printed in U.S.A.

MOLECULAR PHARMACOLOGY

Identification of Tubulin as the Molecular Target of Proapoptotic Pyrrolo-1,5-benzoxazepines

Jude M. Mulligan, Lisa M. Greene, Suzanne Cloonan, Margaret M. Mc Gee, Valeria Onnis, Giuseppe Campiani, Caterina Fattorusso, Mark Lawler, D. Clive Williams, and Daniela M. Zisterer

School of Biochemistry and Immunology, Trinity College, Dublin, Ireland (J.M.M., L.M.G., S.C., V.O., D.C.W., D.M.Z.); Conway Institute of Molecular and Biomedical Research, University College Dublin, Belfield, Dublin, Ireland (M.M.M.); Dipartimento Farmaco Chimico Tecnologico, Universita' degli Studi di Siena, Siena, Italy (G.C., C.F.); and the Institute of Molecular Medicine, St James's Hospital and Trinity College, Dublin, Ireland (M.L.)

Received December 12, 2005; accepted March 29, 2006

ABSTRACT

We have demonstrated previously that certain members of a series of novel pyrrolo-1,5-benzoxazepine (PBOX) compounds potently induce apoptosis in a variety of human chemotherapy-resistant cancer cell lines and in primary ex vivo material derived from cancer patients. A better understanding of the molecular mechanisms underlying the apoptotic effects of these PBOX compounds is essential to their development as antineoplastic therapeutic agents. This study sought to test the hypothesis that proapoptotic PBOX compounds target the microtubules. We show that a representative proapoptotic PBOX compound, PBOX-6, induces apoptosis in both the MCF-7 and K562 cell lines. An accumulation of cells in G_2/M precedes apoptosis in response to PBOX-6. PBOX-6 induces prometaphase arrest and causes an accumulation of cyclin B_1 levels and activation of cyclin B_1/CDK1 kinase in a manner similar to that of two representative antimicrotubule agents, nocodazole and paclitaxel. Indirect immunofluorescence demonstrates that both PBOX-6 and another pro-apoptotic PBOX compound, PBOX-15, cause microtubule depolymerization in MCF-7 cells. They also inhibit the assembly of purified tubulin in vitro, whereas a nonapoptotic PBOX compound (PBOX-21) has no effect on either the cellular microtubule network or on the assembly of purified tubulin. This suggests that the molecular target of the pro-apoptotic PBOX compounds is tubulin. PBOX-6 does not bind to either the vinblastine or the colchicine binding site on tubulin, suggesting that it binds to an as-yet-uncharacterised novel site on tubulin. The ability of PBOX-6 to bind tubulin and cause microtubule depolymerization confirms it as a novel candidate for antineoplastic therapy.

Microtubules are highly dynamic cytoskeletal fibers that are composed of α/β tubulin and play an important role in many physiological processes, especially mitosis and cell division. Their importance in mitosis and cell division makes microtubules an important target for anticancer therapy (Jordan and Wilson, 2004). The well characterized antimitotic drugs that have proven clinical efficacy, such as the taxanes (paclitaxel, docetaxel) and the *Vinca* alkaloids (vincristine, vinblastine, etc.) bind to tubulin. Alternating α- and β-tubulin polymerize to microtubules that constitute the mitotic spindles. Microtubule inhibitors disrupt microtubule dynamics of tubulin polymerization and depolymerization, which results in the inhibition of chromosome segregation in mitosis and consequently the inhibition of cell division. The three major classes of agents that bind tubulin are the taxanes, which stabilize the microtubules by blocking disassembly, the *Vinca* alkaloids, and agents that bind to the colchicine site on tubulin. The latter two classes are microtubule-destabilizing agents that act by blocking assembly of tubulin heterodimers.

In the field of antineoplastic chemotherapy, antimicrotubule agents constitute an important class of compounds, with broad activity both in solid tumors and in hematological

This work was supported financially by Enterprise Ireland and the Higher Education Authority.
Article, publication date, and citation information can be found at http://molpharm.aspetjournals.org.
doi:10.1124/mol.105.021204.

ABBREVIATIONS: JNK, c-Jun-N-terminal kinase; PBOX, pyrrolo-1,5-benzoxazepine; PBOX-6, 7-[(dimethylcarbamoyl) oxy]-6-(2-naphthyl)pyrrolo-[2,1-*d*][1,5]benzoxazepine; PBOX-21, 7-[(diethylcarbamoyl)oxy]-6-p-tolylpyrrolo[2,1-*d*][1,5]benzoxazepine; PBOX-15, pyrrolobenzoxazepine 4-acetoxy-5-(1-(naphthyl)naphtho[2,3-*b*]pyrrolo[2,1-*d*][1,4]oxazepine; FITC, fluorescein isothiocyanate; PARP, poly(ADP-ribose) polymerase; PBS, phosphate-buffered saline; IP, immunoprecipitation; DTT, dithiothreitol; PAGE, polyacrylamide gel electrophoresis; DMSO, dimethyl sulfoxide; PVDF, polyvinylidene difluoride; PIPES, piperazine-*N*,*N*′-bis(2-ethanesulfonic acid); CDK, cyclin dependent kinase.

Downloaded from molpharm.aspetjournals.org at ASPET Journals on June 5, 2017

malignancies. The taxanes are effective in the treatment of refractory ovarian cancer, metastatic breast cancer, non–small-cell lung cancer, and head, neck, and bladder carcinomas (Donaldson et al., 1994; Crown and O'Leary, 2000). The *Vinca* alkaloids have shown clinical benefit in the treatment of leukemia, Hodgkin's disease, non-Hodgkin's lymphomas, testicular cancer, Kaposi's sarcoma, breast cancer, and other malignancies (Jordan and Wilson, 2004). This antineoplastic activity is rooted in these compounds' ability to induce mitotic arrest and subsequent apoptotic cell death via the spindle assembly checkpoint. Antimicrotubule agent-induced mitotic arrest is associated with an up-regulation and activation of cyclin B_1/CDK1 activity in a variety of cell lines (Donaldson et al., 1994). Studies in both normal and transformed human cells treated with antimicrotubule agents have shown that apoptosis can be initiated rapidly and directly from mitotic arrest (Woods et al., 1995; Zhou et al., 2002). In particular, a role for JNK signaling in the apoptotic response of cells to antimicrotubule agents has been suggested. JNK is a member of the mitogen-activated protein kinase family and becomes activated in response to a variety of stressful stimuli, including UV irradiation, growth factor deprivation, heat shock, and chemotherapeutic drugs. JNK activity is also increased by antimicrotubule agents in a wide variety of cell types (Lee et al., 1998; Wang et al., 1998, 1999; Shtil et al., 1999), and inhibition of JNK inhibits paclitaxel- (Lee et al., 1998; Wang et al., 1999), vinblastine- (Brantley-Finley et al., 2003), nocodazole-, and colchicine-induced apoptosis (Wang et al., 1998). Because JNK has been implicated primarily in stress responses, JNK activation by antimicrotubule agents may represent an acute response to microtubule damage. The phosphorylation and thus inactivation of the antiapoptotic protein Bcl-2 has also been described as an important step from microtubule damage to apoptosis induction (Blagosklonny et al., 1997), and many studies have implicated JNK in the upstream signaling pathway leading to Bcl-2 phosphorylation (Srivastava et al., 1999).

We have previously demonstrated, in a series of articles, that certain members of a novel series of PBOX compounds (Fig. 1) potently induce apoptotic cell death in a variety of human chemotherapy-resistant cancer cell lines, indicating their potential in the treatment of both solid tumors and tumors derived from the hematopoietic system (Zisterer et al., 2000; Mc Gee et al., 2002a,b, 2004). Dissecting the molecular mechanisms underlying PBOX-induced apoptosis is fundamental to their development as therapeutic agents in the treatment of cancer. We have shown that activation of JNK is essential during PBOX-induced apoptosis (Mc Gee et al., 2002a) and that Bcl-2 phosphorylation is a critical step in the apoptotic pathway induced by a representative PBOX compound, PBOX-6 (Mc Gee et al., 2004). In the present study, we examine the hypothesis that PBOX compounds are microtubule-targeting drugs. We show that PBOX-6 causes an up-regulation in CDK1 activity before apoptosis. Indirect immunofluorescence analysis demonstrates that pro-apoptotic PBOX compounds cause a depolymerization of the microtubule network and inhibit assembly of purified tubulin in vitro. This study identifies tubulin as the molecular target of the proapoptotic PBOX compounds.

Materials and Methods

Materials. MCF-7 human breast carcinoma breast cells were obtained from the European Collection of Cell Cultures (Porton Down, Wiltshire, UK). The pyrrolobenzoxazepines 7-[(dimethylcarbamoyl) oxy]-6-(2-naphthyl)pyrrolo-[2,1-*d*][1,5]benzoxazepine (PBOX-6), 7-[(diethylcarbamoyl)oxy]-6-p-tolylpyrrolo[2,1-*d*][1,5]benzoxazepine (PBOX-21), and pyrrolobenzoxazepine 4-acetoxy-5-(1-(naphthyl)naphtho[2,3-*b*]pyrrolo[2,1-*d*][1,4]oxazepine (PBOX-15) were synthesized as described previously (Campiani et al., 1996) The ApopTag Plus Kit was obtained from Chemicon International Inc. (Temecula, CA), the RapiDiff kit was obtained from Diagnostic Developments (Burscough, Lancashire, UK), and the CytoDYNAMIX Screen3 was obtained from Cytoskeleton Inc. (Denver, CO). Colchicine, nocodazole, paclitaxel, vincristine, and vinblastine were purchased from Sigma (Poole, Dorset, UK). [^{3}H]Vinblastine was prepared by Amersham Biosciences (Buckinghamshire, UK), and the fluorescein-labeled colchicine was obtained from Cytoskeleton, Inc. The PBOX compounds were dissolved in ethanol, whereas the remaining drugs were dissolved in dimethyl sulfoxide. Control samples were prepared with equivalent volumes of the appropriate solvent. Anti-α-tubulin and FITC-conjugated goat anti-mouse antibodies were purchased from Sigma, anti-cyclin A, anti-cyclin B_1, and anti-CDK1 antibodies were obtained from BD Pharmingen (Cowley, Oxford, UK). Anti-JNK antibody was purchased from Santa Cruz Biotechnology (Heidelberg, Germany), and anti-PARP antibody was obtained from Merck Biosciences (Beeston, Nottingham, UK). Histone H1 and glutathione-*S*-transferase–c-Jun substrates were purchased from Sigma and Cell Signaling Technology Inc. (Beverly, MA) respectively. The ECL detection system and [γ^{32}P]ATP were purchased from Amersham Biosciences (Little Chalfont, Buckinghamshire, UK). Unless stipulated, all other reagents were purchased from Sigma.

Cell Culture. MCF-7 and K-562 cells were grown at 37°C under a humidified atmosphere of 95% O_2 and 5% CO_2. The MCF-7 cells were maintained in minimum essential medium, whereas the K562 cells were maintained in RPMI 1640 medium. Both media were supplemented with 10% (v/v) fetal calf serum, 2 mM L-glutamine and 100 μg/ml gentamicin (complete medium). The minimum essential medium was also supplemented with 1% (v/v) nonessential amino acids.

Flow Cytometric Analysis. Cells were harvested by trypsinization and after centrifugation were washed with PBS and incubated in ice-cold 70% ethanol in PBS at 4°C. The samples were then centrifuged to remove the ethanol, resuspended in 1 ml of staining solution (10 μg/ml RNase A and 100 μg/ml propidium iodide) and incubated in the dark for 30 min at 37°C. Flow cytometric analysis was performed using a FACSCalibur flow cytometer and CellQuest software (BD Biosciences, San Jose, CA).

RapiDiff Staining of Cells. MCF-7 cells were seeded at a density of 1×10^5 in a volume of 1 ml per well of a 24-well plate. After treatment with the indicated compounds, a 500-μl aliquot of the cells was treated with 1 mM EDTA to prevent clumping of the cells. The cells were then resuspended thoroughly and cytocentrifuged on to poly-L-lysine-coated slides at 700*g* for 2 min. The slides were stained with the RapiDiff kit (eosin/methylene blue) under conditions described by the manufacturer.

Immunoprecipitation and Kinase Activity Assays. Cells were lysed in IP lysis buffer containing 50 mM HEPES, pH 7.5, 150 mM NaCl, 1 mM EDTA, 2.5 mM EGTA, 10% (v/v) glycerol, 0.1% (v/v) Tween 20, 1 mM DTT, 1 mM NaF, 10 mM β-glycerophosphate, and protease inhibitors (10 μg/ml leupeptin, 10 μg/ml aprotinin, 0.1 mM phenylmethylsulfonyl fluoride, and 0.1 mM sodium orthovanadate). The DTT, NaF, β-glycerophosphate, and protease inhibitors were added fresh to the IP buffer. The protein content of the supernatant was determined by Bradford assay (Bio-Rad Laboratories, Hercules, CA). The appropriate antibody (1 μg) was added to equal amounts of protein (100–500 μg) in each cell lysate sample. The samples were

Downloaded from molpharm.aspetjournals.org at ASPET Journals on June 5, 2017

incubated for 3 h at 4°C. A 50% slurry of protein A beads in PBS (50 μl) was then added to the samples and incubated overnight at 4°C. The samples were then centrifuged for 2 min at 500*g*, and the beads were washed. The precipitates were washed three times in 1 ml of ice-cold IP lysis buffer and then used either for kinase activity assay or resuspended in 20 μl of 3× SDS sample buffer and resolved by SDS-PAGE for Western blot analysis. For kinase activity assays, after washes with ice-cold IP lysis buffer, the immune-complex beads were washed three times with ice-cold kinase buffer that contained 50 mM HEPES, pH 7.5, 2.5 mM EGTA, 10 mM $MgCl_2$, 1 mM DTT, 10 mM β-glycerophosphate, 1 mM NaF, and 0.1 mM sodium orthovanadate. The kinase reactions were performed by incubating the immunoprecipitates in 30 μl of kinase buffer supplemented with 20 μM unlabeled ATP, 2 μCi of [γ^{32}P]ATP, and either 10 μg of Histone H1 substrate for CDK1 or 1 μg of glutathione-*S*-transferase–c-Jun substrate for JNK1, and incubating them at 30°C for 30 min. The kinase reactions were stopped by resuspending the samples in an aliquot of 3× SDS sample buffer (20 μl) and resolved by SDS-PAGE. The gel was dried under a vacuum and exposed to Kodak X-Omat film at −70°C. Phosphorylation was quantitated by densitometric scan analysis (using Scion Image; Scion Corp, Frederick, MD) of the phosphorylated bands in the autoradiogram.

Western Blot Analysis. Cells were lysed in lysis buffer containing 50 mM Tris-HCl, pH 7.5, 250 mM NaCl, 5 mM EDTA, 0.1% (v/v) Triton, 50 mM sodium fluoride, protease inhibitors (1 μg/ml aprotinin, 1 μg/ml leupeptin, 1 μg/ml pepstatin A, 1 mM sodium orthovanadate, and 100 μg/ml phenylmethylsulfonyl fluoride), and 1 mM DTT, and the protein concentration of the resultant supernatants were determined by a Bradford assay. For Western blot analysis of PARP, the cells were resuspended in 200 μl of PARP sample buffer [62.5 mM Tris-HCL, pH 6.8, 6 M urea, 10% (v/v) glycerol, 2% (w/v) SDS, 0.00125% bromphenol blue, and 5% (v/v) β-mercaptoethanol added immediately before use], sonicated for 15 s, and heated at 65°C for 15 min. Equal amounts of lysate was resolved by SDS-PAGE and transferred onto 0.2-μm PVDF membrane. The PVDF membrane was blocked in blocking buffer containing 5% (w/v) dry milk in 0.1% (v/v) Tween 20 in Tris-buffered saline at room temperature for 1 to 3 h. After blocking of the membrane, the immunoblot was incubated in primary antibody overnight at 4°C and in horseradish peroxidase-labeled secondary antibody for 1 h at room temperature according to manufacturer's instructions. The immunoblots were analyzed using the ECL detection system.

Indirect Immunofluorescence. Cells seeded upon coverslips were washed gently with 1 ml of PBS and fixed in 100% methanol at −20°C for 10 min, after which time they were washed three times with PBS. The cells were then blocked at room temperature for 30 min in 5% bovine serum albumin made up in 0.1% (v/v) Triton X-100 in PBS. The cells were incubated for 1 h at room temperature in primary antibody to α-tubulin, washed three times with PBS, and then incubated for a further hour at room temperature in FITC-conjugated goat anti-mouse secondary antibody, after which time they were washed a further three times with PBS. The cells were then incubated with 0.2 μg/ml propidium iodide made up in blocking buffer for 2 min. To each coverslip, 5 μl of a 2 μg/ml phenylethylene diamine in a 50:50 solution of PBS and glycerol was applied to the surface of each slide. The slides were then immediately mounted and viewed at a magnification of 1000× with a Nikon microscope, and images were captured using ImageCapture software.

Tubulin Polymerization Assay. The assembly of >99% purified bovine tubulin was monitored using the CytoDYNAMIX Screen 3. Purified bovine brain tubulin was resuspended on ice in ice-cold buffer [80 mM PIPES, pH 6.9, 0.5 mM $MgCl_2$, 1 mM EGTA, and 1 mM GTP, 5% (v/v) glycerol], and a 100-μl volume (300 μg) was pipetted into the designated wells of a half-area 96-well plate prewarmed to 37°C. Each compound tested was made up in the same buffer. The assay was conducted at 37°C and tubulin polymerization was followed turbidimetrically at 340 nm in a Spectramax 340PC spectrophotometer (Molecular Devices, Sunnyvale, CA). The absorbance was measured at 30-s intervals for 1 h.

Colchicine Tubulin Competition Binding Assay. Each reaction was performed in 0.25 mM PIPES buffer at pH 6.9, containing 0.05 mM GTP, 0.25 mM $MgCl_2$, test compound at the appropriate concentration, and >99% purified tubulin stock (1 mg/ml). The reaction mixture was mixed gently and incubated at 37°C for 30 min, after which time fluorescent colchicine was added to each reaction, giving a final concentration of 0.5 μM. This was then incubated for a

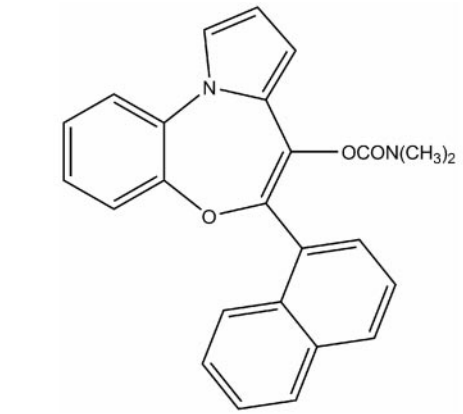

PBOX-6

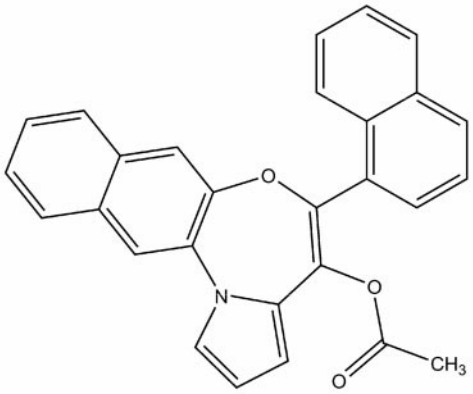

PBOX-15

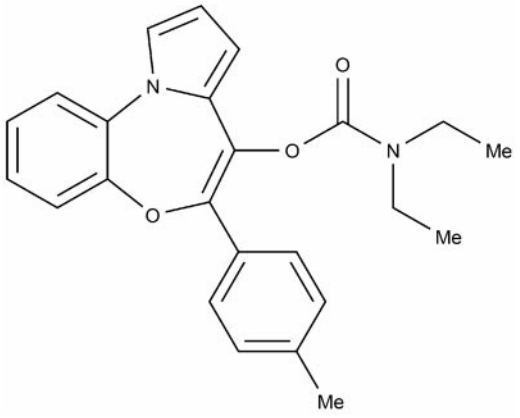

PBOX-21

Fig. 1. Structures of pyrrolo-1,5-benzoxazepine (PBOX) compounds.

Downloaded from molpharm.aspetjournals.org at ASPET Journals on June 5, 2017

further 30 min at 37°C. Each reaction was then applied to a G25 Sephadex chromatography column, and the eluate from the columns was collected in designated wells of a 96-well plate. When the eluate from the application of the reaction mixture had been collected, 160 μl of buffer was applied to the top of the column, and the eluate was collected in a fresh well. This was continued until 12 wells were filled for each reaction. The plate was then read on a Spectramax Gemini XS fluorescence 96-well spectrophotometer (Molecular Devices) at excitation and emission wavelengths of 485 and 535 nm, respectively.

Vinblastine Tubulin Competition Binding Assay. The ability of a ligand to bind to the vinblastine-binding site on tubulin was assayed as described for determination of binding to the colchicine-binding site, using a radiolabeled instead of a fluorescent analog. The binding of radiolabeled [^{3}H]vinblastine was used, and its presence within the collected fractions was measured by liquid scintillation counting. Each reaction contained a final concentration of 0.5 μM [^{3}H]vinblastine and >99% purified bovine brain tubulin (1 mg/ml). The separation of the bound [^{3}H]vinblastine from unbound [^{3}H]vinblastine was achieved using a G50 Sephadex column.

Results

PBOX-6 Induced Apoptosis Is Preceded by an Accumulation of Cells in G_2/M. Microtubule-targeting drugs have been shown to induce G_2/M arrest and apoptosis in many human tumor cells. Figure 2 demonstrates that PBOX-6 (Fig. 1)-induced apoptosis (as measured by the pre-G_1 peak in fluorescence-activated cell sorting analysis) of human breast MCF-7 and chronic myelogenous leukemia K562 cells was preceded by an accumulation of cells in the G_2/M phase. Terminal deoxynucleotidyl transferase dUTP nick-end labeling and PARP cleavage confirmed that the PBOX-6 induced increase in the pre-G_1 peak was due to apoptotic cell death (results not shown). This detailed time course of the changes in distribution of cell cycle phases in response to PBOX-6 treatment also demonstrated that PBOX-6–induced apoptosis was temporally preceded by arrest in the G_2/M phase of the cell cycle.

PBOX-6 Induces Morphological Features of Prometaphase Arrest in MCF-7 Cells. Microtubule targeting agents are known to arrest the cell cycle in early mitosis (i.e., prometaphase/metaphase). The morphological features of MCF-7 cells were analyzed after treatment with PBOX-6 and compared with two representative antimicrotubule agents, paclitaxel and nocodazole, as controls (Fig. 3). Cells treated with either of the compounds displayed distinct signs of arrest in the prometaphase stage of mitosis as the nuclear membrane disappeared and the chromatin was condensed. This suggests that the PBOX-6 acted as a mitotic inhibitor. Similar results were obtained in K562 cells, indicating that prometaphase arrest induced by PBOX-6 was not restricted to MCF-7 cells (data not shown).

Downloaded from molpharm.aspetjournals.org at ASPET Journals on June 5, 2017

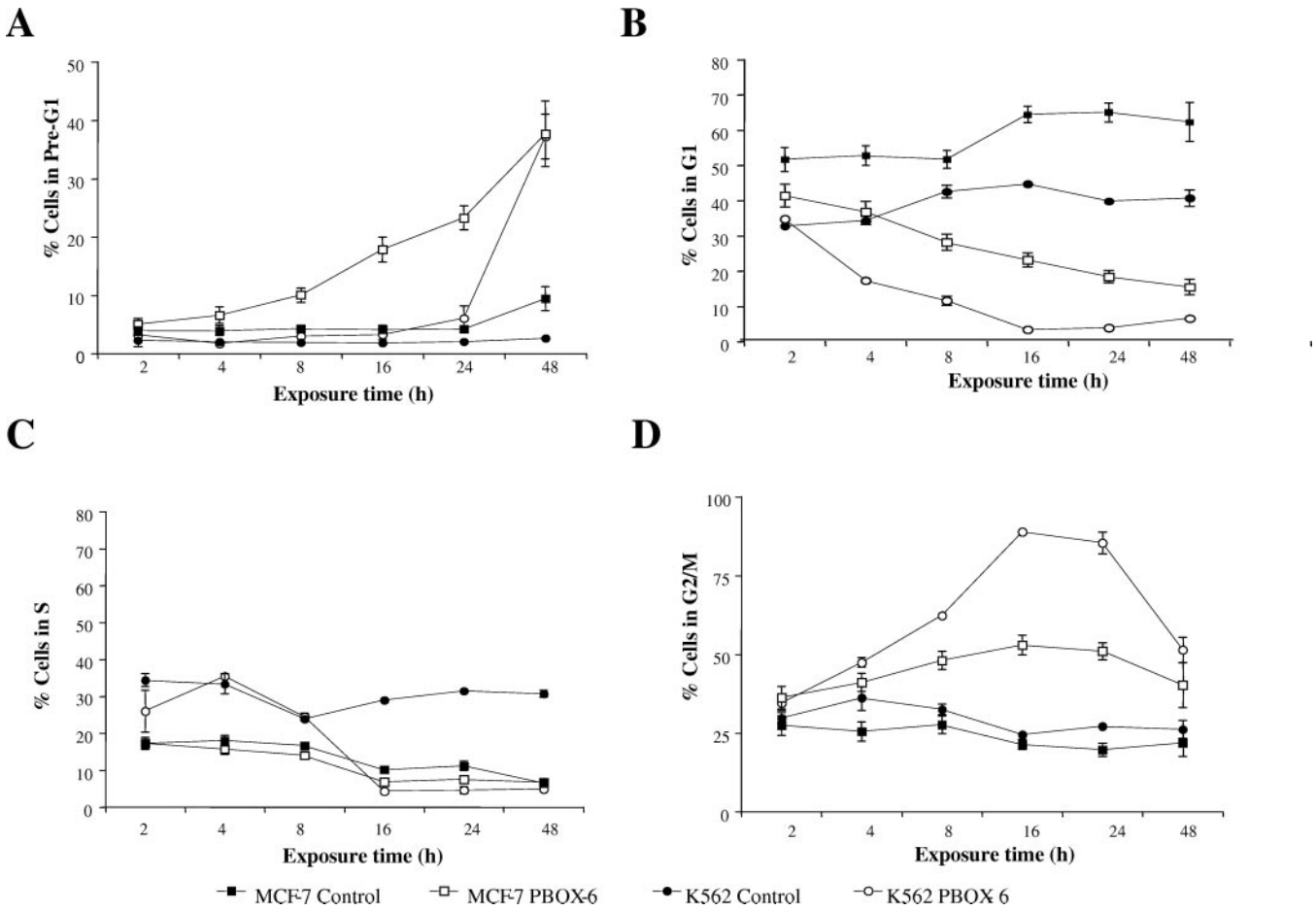

Fig. 2. PBOX-6-induced apoptosis is accompanied by G_2/M arrest. MCF-7 and K562 cells were treated either with vehicle [0.5% (v/v) ethanol (Control)] or 10 μM PBOX-6 for up to 48 h. Cells were harvested at the time points indicated as described under *Materials and Methods*, and the percentage of cells in each phase of the cell cycle [pre-G_1 phase (A), G_1 phase (B), S phase (C), and G_2/M phase (D)] was analyzed using flow cytometry. The pre-G_1 phase represents apoptotic cells. The results represent the mean ± S.E.M of six separate experiments.

Effect of PBOX-6 on Cyclin B_1 Expression and CDK1 Activity. It was next necessary to determine what effect PBOX-6 treatment had upon CDK1 kinase activity, because it is responsible, through association with its cyclin partner, cyclin B_1, for driving the cell through G_2 and mediating both entrance into and exit out of the M phase of the cell cycle. Paclitaxel and nocodazole-induced M-phase arrest is associated with up-regulation and activation of cyclin B/CDK1 kinase in a variety of cell lines (King et al., 1994; Wang et al., 1998); thus, treatment with these drugs served as a positive control. Treatment with PBOX-6, paclitaxel, or nocodazole resulted in a time-dependent increase in CDK1 kinase activity relative to the vehicle control (Fig. 4, A, B, and C, respectively). To address the mechanism by which CDK1 activity was being stimulated, the expression levels of both CDK1 and the cyclins known to associate with it, namely cyclin A and B_1, were determined. There was no alteration in protein expression of either cyclin A or CDK1 before or coincident with the increase in CDK1 activity after treatment with any of the compounds (results not shown). Analysis of expression of cyclin B_1, however, did reveal a marked increase in cyclin B_1 after treatment with either PBOX-6 (Fig. 5A), paclitaxel, or nocodazole (Fig. 5B), which directly correlated with the increase in CDK1 activity for each of these compounds (see Fig. 4). Immunoprecipitation experiments confirmed that the PBOX-6 induced CDK1 activity was associated with cyclin B_1 (data not shown). Similar results were also obtained in K562 cells, indicating that the activation of cyclin B_1/CDK1 kinase caused by PBOX-6 is not restricted to MCF-7 cells (data not shown). Induction of cyclin B_1/CDK1 kinase activity is a hallmark associated with mitotic arrest, confirming the suggestion that PBOX-6 arrests cells in the G_2/M phase of the cell cycle.

PBOX-6 Causes a Dose-Dependent Disruption of MCF-7 Cellular Microtubule Network. Antimicrotubule agents are known to target the cellular microtubule network, resulting in aberrant formation of the mitotic spindle, subsequent blockage of the cell cycle in G_2/M phase, and apoptotic cell death (Wassmann and Benezra, 2001). Because PBOX-6 markedly blocked the cell cycle in M phase and induced apoptotic cell death, we tested whether PBOX-6 could directly affect the organization of the microtubule network of cells. MCF-7 cells were treated with either a range of concentrations of PBOX-6 (100 nM to 10 μM), paclitaxel (1 μM), nocodazole (1 μM), or with the same volume of vehicle as control. After 16 h of incubation, the microtubule network was visualized by indirect immunofluorescence. The microtubule network in control cells exhibited normal arrangement with microtubules seen to traverse intricately throughout the cell, and these cells displayed a normal compact rounded nucleus (Fig. 6A). In contrast, PBOX-6 caused a dose-dependent loss of microtubule network, with only a diffuse stain visible throughout the cytoplasm (Fig. 6, B–D). These effects are similar to that exerted by nocodazole (Fig. 6E) a known microtubule depolymerizer. Paclitaxel, on the other hand, exerts its effects by stabilizing the microtubule

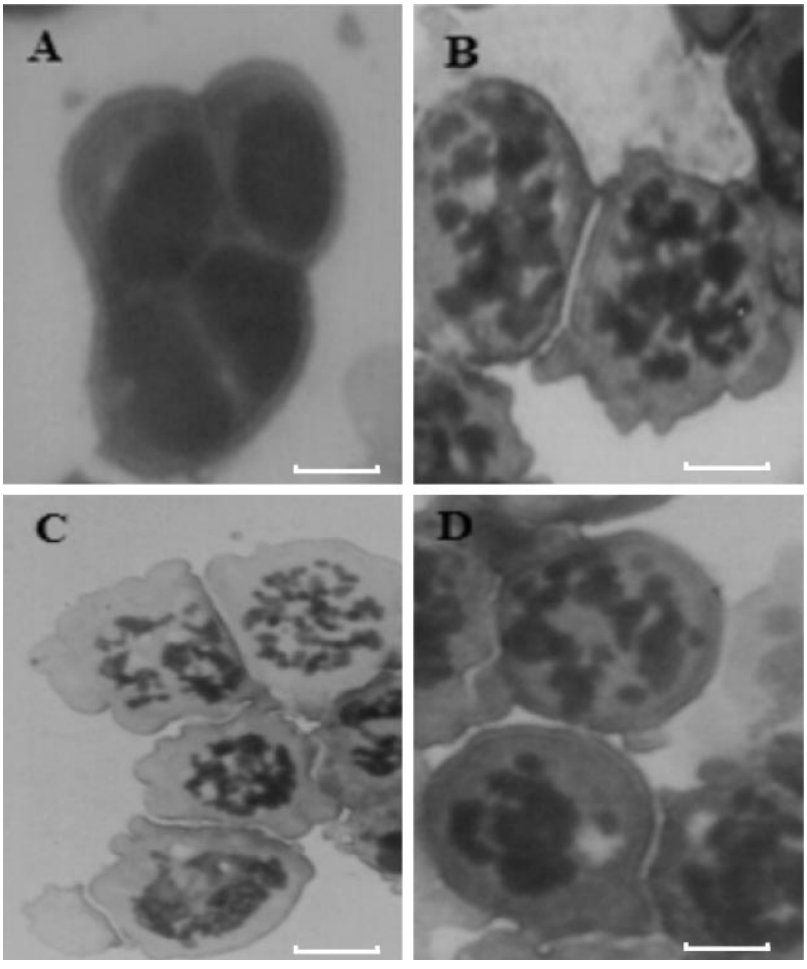

Fig. 3. PBOX-6 treatment induces morphological features of prometaphase arrest in MCF-7 cells. Microscopic analysis of MCF-7 cells was performed after treatment with either vehicle [0.5% (v/v) ethanol (A)], 10 μM PBOX-6 (B), 10 μM nocodazole (C), or 10 μM paclitaxel (D) for 8 h. After treatment, cells were centrifuged onto a glass slide and stained using the Rapi Diff kit. The cells were visualized under a light microscope (Nikon) at a magnification of 40×. Scale bar, 10 μm. The results shown are representative of three separate experiments.

Downloaded from molpharm.aspetjournals.org at ASPET Journals on June 5, 2017

network, and resulted in a distinctive rigidity of the microtubules causing them to form microtubule 'bundles' (Fig. 6F).

PBOX-21 (Fig. 1) is a nonapoptotic member of the PBOX series of compounds and in fact induces G_1 arrest within MCF-7 cells with no associated cytotoxicity (Mulligan et al., 2003). To test the hypothesis that the differential response of the non- and proapoptotic subsets of PBOX compounds is based upon their ability to disrupt the microtubule network,

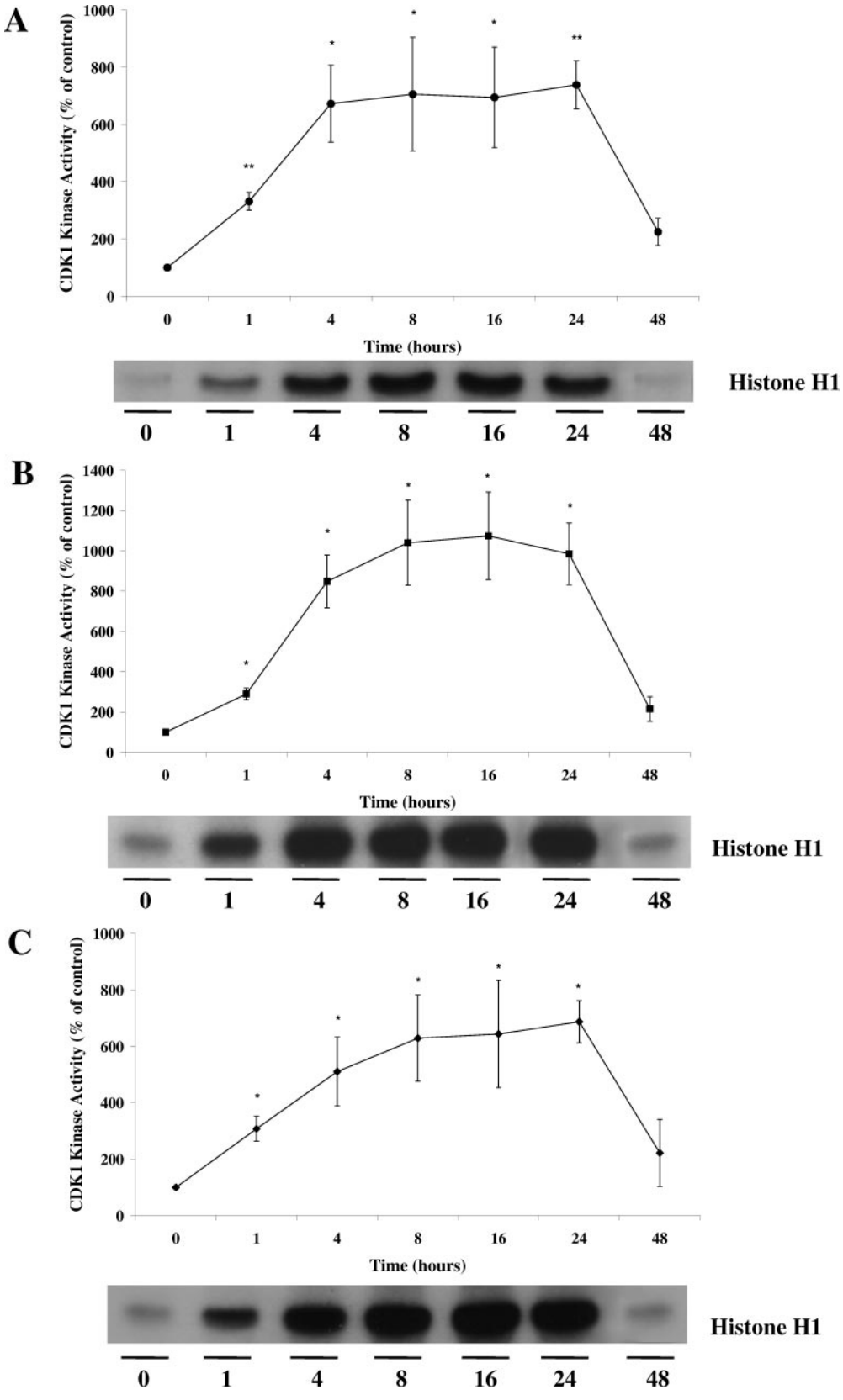

Fig. 4. PBOX-6 induces an up-regulation in CDK1 kinase activity in a manner comparable with paclitaxel and nocodazole. Whole-cell extracts were prepared from MCF-7 cells after treatment with either 10 μM PBOX-6 (A), paclitaxel (B), or nocodazole (C) for the indicated times. Protein (200–500 μg) was immunoprecipitated with anti-CDK1 antibody and protein A beads and then incubated with Histone H1 substrate and [γ-^{32}P]ATP and resolved by SDS-PAGE. Densitometry was performed on the resultant bands using Scion Image software with the 0-h vehicle control set to 100%. The results represent the mean ± S.E.M of three separate experiments. Statistical analysis was carried out using Excel (Microsoft Corp., Redmond, WA). * $p < 0.05$, **, $p < 0.01$ with respect to 0-h vehicle, Student's t test.

Downloaded from molpharm.aspetjournals.org at ASPET Journals on June 5, 2017

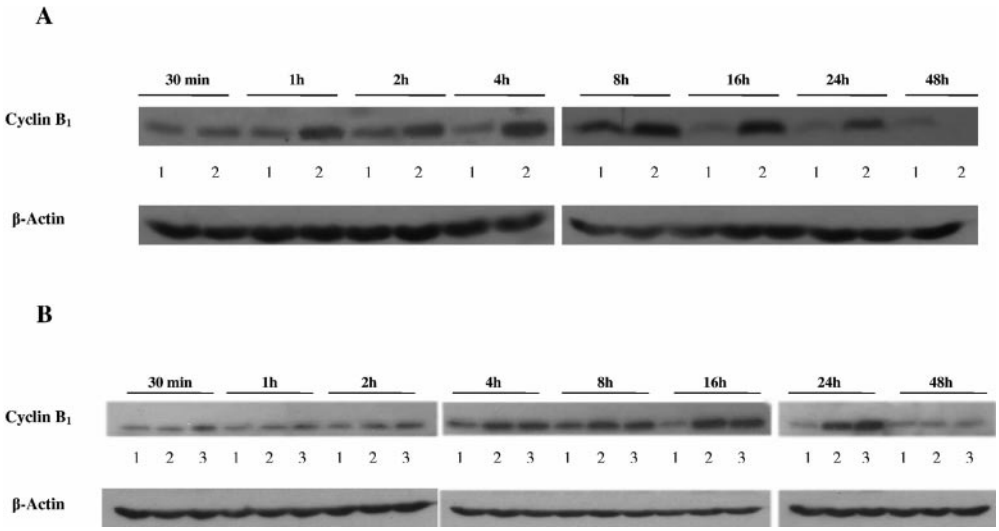

Fig. 5. PBOX-6 induces an up-regulation in cyclin B_1 expression in a manner comparable with paclitaxel and nocodazole. Whole-cell extracts were prepared from MCF-7 cells after treatment with either vehicle [0.5% (v/v) ethanol (1)] or 10 μM PBOX-6 (2) for the indicated times. Protein (50 μg) was resolved using SDS-PAGE, transferred onto PVDF, and probed with anti-cyclin B_1 antibody (A). Results were compared with an immunoblot of samples prepared from MCF-7 cells after treatment with either vehicle [0.5% (v/v) DMSO (1)], paclitaxel (2), or nocodazole (3) for the indicated times (B). The results shown are representative of four separate experiments.

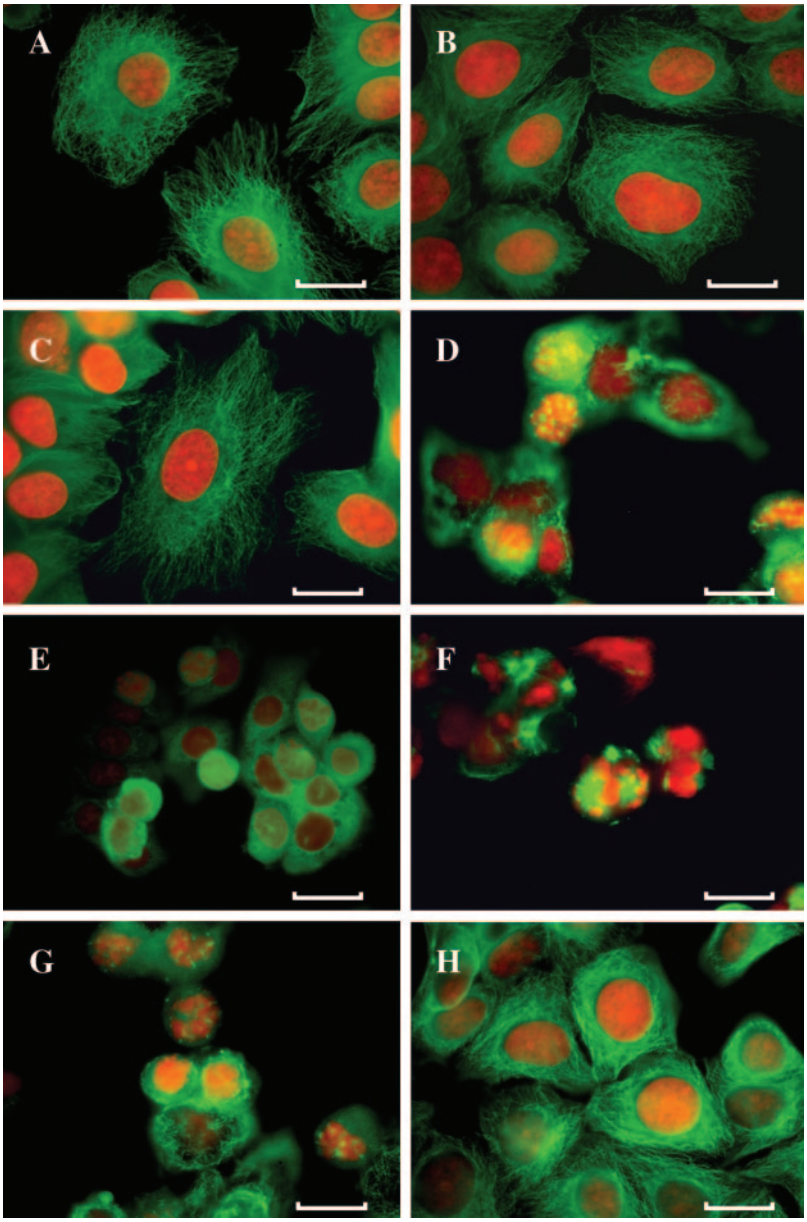

Fig. 6. Effect of PBOX-6, PBOX-15, PBOX-21, paclitaxel, and nocodazole upon the organization of MCF-7 cellular microtubule network. MCF-7 cells were treated with either vehicle [0.5% (v/v) ethanol] (A), 100 nM, 1 μM, or 10 μM PBOX-6 (B, C, and D, respectively), 1 μM nocodazole (E), 1 μM paclitaxel (F), 1 μM PBOX-15 (G), or 25 μM PBOX-21 (H) for 16 h. After this time, the medium was carefully removed and the cells fixed in ice-cold methanol. Cells were incubated with monoclonal anti-α-tubulin antibody for 1 h at room temperature, and then incubated with FITC-conjugated anti-mouse secondary antibody for a further hour at room temperature. After washing, the cells were stained briefly with propidium iodide. The organization of the microtubule network (green) and the cellular DNA (red) was visualized by Nikon PS200 fluorescence microscopy at a magnification of 100×. Scale bar, 10 μm. The results shown are representative of three separate experiments.

Downloaded from molpharm.aspetjournals.org at ASPET Journals on June 5, 2017

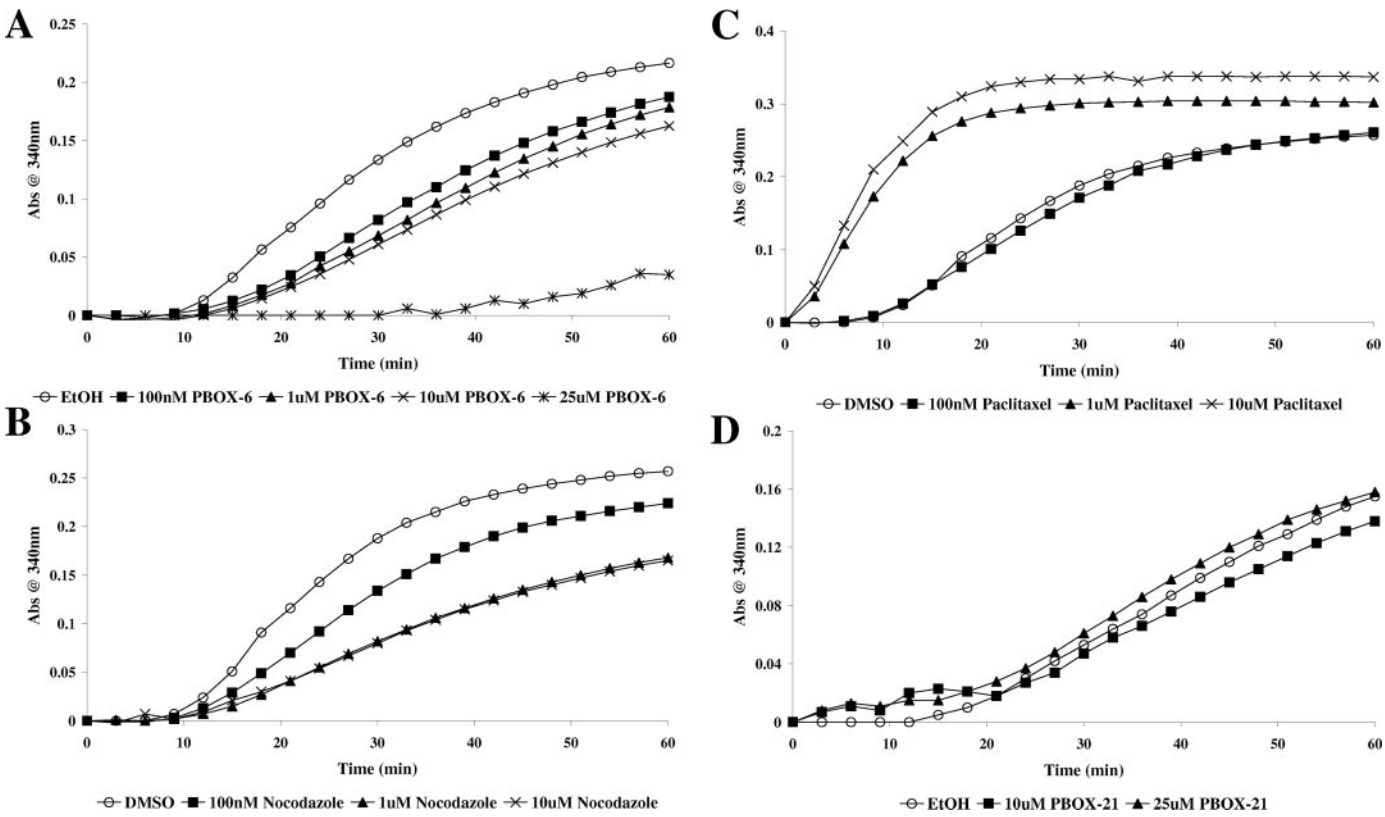

Fig. 7. PBOX-6 causes a dose-dependent depolymerization of tubulin, whereas PBOX-21 has a negligible effect upon polymerization status of tubulin. Purified bovine tubulin was incubated at 37°C in the presence of either vehicle [0.5% (v/v) ethanol or DMSO] or the indicated concentrations of PBOX-6 (A), nocodazole (B), paclitaxel (C), or PBOX-21 (D). Tubulin polymerization was determined by measuring the increase in absorbance over time at 340 nm. The results shown are representative of three separate experiments.

the effect of PBOX-21, as well as a second potent proapoptotic PBOX compound, PBOX-15 (Fig. 1), on the microtubule network of MCF-7 cells was examined. It was found that, similar to PBOX-6 (10 μM), PBOX-15 (1 μM) (Fig. 6G) seemed to induce a loss of the microtubule network of the cell. On the other hand, PBOX-21 (25 μM) (Fig. 6H), had no effect upon the MCF-7 microtubule network and, as such, PBOX-21 may be considered a negative control. Together, these results indicate that the microtubule was the intracellular target for proapoptotic PBOX compounds such as PBOX-6.

Effect of PBOX-6 on Tubulin Polymerization in Vitro. Because PBOX-6 markedly disrupted the cellular microtubule network, we tested whether PBOX-6 could directly affect tubulin, the main component of this network. To test this hypothesis, tubulin polymerization and depolymerization in vitro were studied at 37°C in a reaction mixture containing purified tubulin and GTP. Results presented in Fig. 7A show that PBOX-6 inhibited the polymerization of tubulin in a dose-dependent manner, similar to the effect elicited by nocodazole (Fig. 7B). Similar results were obtained with the other representative proapoptotic PBOX compound, PBOX-15 (data not shown). As in previous reports, paclitaxel was shown to promote tubulin polymerization in a concentration-dependent manner (Fig. 7C). In contrast, PBOX-21 was found to have a negligible effect upon the polymerization of tubulin in vitro relative to the vehicle control (Fig. 7D), in agreement with its lack of effect upon the cellular microtubule network. This again distinguishes the mechanism of action of the non- and proapoptotic subsets of the PBOX compounds and identifies tubulin as the molecular target of the proapoptotic PBOX members.

Lack of Binding of PBOX-6 to the Vinblastine- and Colchicine-Binding Sites on Tubulin. Because PBOX-6 has been shown to directly bind to and cause depolymerization of purified tubulin, it was necessary to gain information about the binding site of PBOX-6 on tubulin. To date, only the binding sites of the depolymerizers colchicine (Serrano et al., 1984; Uppuluri et al., 1993; Ravelli et al., 2004) and vinblastine (Rai and Wolff, 1996) on tubulin have been well characterized. Compounds capable of depolymerizing tubulin may bind to either of these two sites, or to an as-yet-uncharacterized novel site on tubulin. Assessment of the binding of PBOX-6 to the colchicine-binding site involved a fluorescence-based assay. Excess unlabeled colchicine (100 μM) or nocodazole (10 μM), which is known to bind to the colchicine-binding site (Friedman and Platzer, 1978; Uppuluri et al., 1993), displaced the binding of fluorescently labeled colchicine relative to the vehicle control (Fig. 8A). PBOX-6 at a concentration of 10 μM, however, did not displace the binding of labeled colchicine, suggesting that PBOX-6 does not bind to the colchicine-binding site on tubulin.

Next, we determined the ability of PBOX-6 to bind to the vinblastine-binding site on tubulin using a [^{3}H]vinblastine displacement assay. As expected, excess unlabeled vinblastine (100 μM) and also vincristine (10 μM) (which binds to the vinblastine-binding site) were able to displace [^{3}H]vinblastine relative to their vehicle control [0.5% DMSO (v/v)], causing a reduction in the radioactive signal in the fractions

Downloaded from molpharm.aspetjournals.org at ASPET Journals on June 5, 2017

containing tubulin (i.e., fractions 5–9) (Fig. 8B). In contrast, 10 μM PBOX-6 did not cause a reduction of the radioactive signal relative to the PBOX-6 vehicle control in the fractions containing tubulin, suggesting that PBOX-6 did not bind to the vinblastine-binding site. Any residual [^{3}H]vinblastine that did not bind tubulin, or [^{3}H]vinblastine that had been displaced from binding to tubulin by a vinblastine-binding site competitor, was seen to elute between fractions 10 and 30. These combined results from the colchicine and vinblastine displacement assays indicate that PBOX-6 did not bind to the known sites and might have its own novel binding on tubulin.

Discussion

Although it is a potent member of a novel series of PBOX compounds, PBOX-6 has previously been shown to induce apoptosis in many human tumor cell lines, our knowledge of the mechanism of action by which PBOX-6 induces apoptosis remained incomplete. We have shown previously that activation of JNK is essential during PBOX-induced apoptosis (Mc Gee et al., 2002a) and that Bcl-2 phosphorylation is a critical step in the apoptotic pathway induced by a PBOX-6 (Mc Gee et al., 2004), but the molecular target of PBOX-6 remained to be identified. The present study demonstrates that apoptosis induced by PBOX-6 in human MCF-7 and K562 cells is preceded by a marked G_2/M arrest. The cells displayed morphological features that identified a mitotic arrest, specifically in prometaphase. During prometaphase, the DNA chromatin network, which was duplicated in the S period of interphase, begins to twist and fold, eventually forming compacted chromosomes. The nuclear envelope breaks down, allowing the nucleoplasmic contents to come into contact with the spindle network, as the cell prepares to align its duplicated chromosomes during metaphase for separation by the mitotic spindle during anaphase (Crespo et al., 2001). The morphological effects elicited by PBOX-6 were similar to that initiated by two microtubule-targeting drugs, paclitaxel and nocodazole, a representative polymerizer and depolymerizer, respectively. This is in agreement with previous reports, which show that antimicrotubule agents arrest the cell cycle in prometaphase (Woods et al., 1995; Li and Broome, 1999).

In eukaryotic cells, cell cycle progression is regulated through the activation and inactivation of cyclin-dependent kinases, cyclins, and other regulatory factors. Inappropriate

MOL Manuscript # 21204

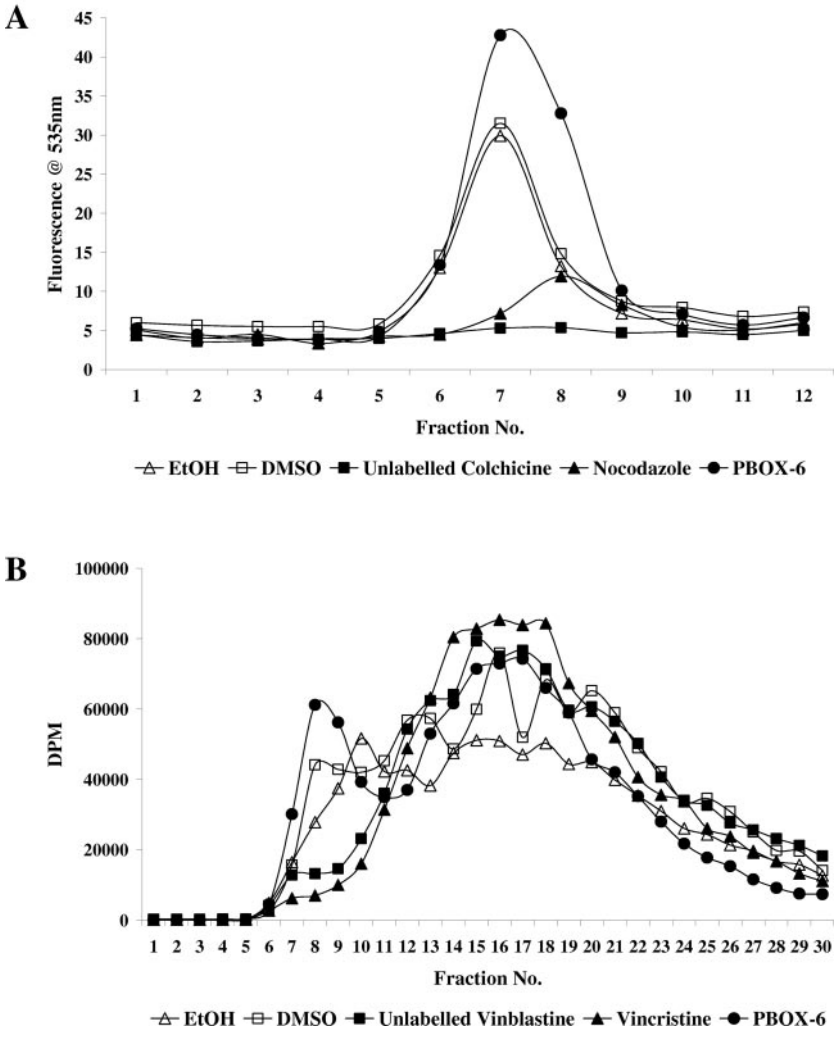

Fig. 8. PBOX-6 does not bind to the colchicine- or vinblastine-binding site on purified tubulin. Each reaction mixture contained 1 mg/ml 99% purified bovine tubulin, 0.25 mM PIPES buffer at pH 6.9, containing 0.05 mM GTP, and 0.25 mM $MgCl_2$, in the presence or absence of either excess unlabeled colchicine (100 μM) (A) or vinblastine (B). The colchicine and vinblastine binding assays were performed as described under *Materials and Methods*. Each reaction mixture contained either 0.5 μM FITC-labeled colchicine (A) or 0.5 [^{3}H]vinblastine (B) and was incubated for 30 min at 37°C. When evaluating the ability of a test compound to bind to either of these sites, the reaction was performed in the presence or absence of the indicated test compounds (10 μM) or the appropriate vehicle control (ethanol for PBOX-6 and DMSO for the other compounds). The data presented are representative of two separate experiments.

Downloaded from molpharm.aspetjournals.org at ASPET Journals on June 5, 2017

alteration in the expression and/or activation of cyclin-dependent kinases and regulators can lead to blockade of cell cycle progression and induction of apoptosis. It has been widely reported that cyclin B_1/CDK1 complexes are involved in the regulation of the G_2/M phase and the M-phase transition. Many reports have demonstrated that antimicrotubule drug-induced M-phase arrest, inappropriate accumulation of B-type cyclins and activation of CDK1 were associated with the initiation of apoptotic pathways. In the present study, we show that PBOX-6 treatment promoted an increase in cyclin B_1 protein levels and stimulation of CDK1 activity with a pattern similar to that detected for both paclitaxel and nocodazole. The G_2/M arrest profile paralleled the induction of cyclin B_1 expression and CDK1 activity after treatment with PBOX-6, which suggests that sustained activation of CDK1 kinase activity by this compound is essential for the cessation of the cell cycle at the G_2/M phase.

PBOX-6 was found to induce many of the hallmarks associated with mitotic arrest in a manner similar to that of antimicrotubule agents, which suggested that PBOX-6 might possess antimicrotubule activity. This hypothesis was tested by assessing the ability of PBOX-6 to interact with the microtubule network of the cell. Indirect immunofluorescence allowed visualization of both the microtubule network and the DNA of the cell. This technique allowed detection of morphological changes in the microtubule network, such as alterations in microtubule organization and arrangement. It also allowed for detection of disruption to the DNA of the cell. It revealed that PBOX-6 possesses antimicrotubule activity, in that PBOX-6 treatment disrupted the microtubule network of the cell in a dose-dependent manner. This is in agreement with the dose-dependent induction of mitotic arrest and apoptosis already observed and suggests that these effects are a direct result of the PBOX-6-mediated abrogation of the microtubule network of the cell. The disruption to the microtubules after treatment with 10 μM PBOX-6 was similar to that elicited by the known microtubule depolymerizer nocodazole. Increasing concentrations of nocodazole and other known tubulin depolymerizers are known to kinetically 'cap' the actively growing plus end of microtubules, preventing growth and thus leading ultimately to disassembly of the microtubules (Dumontet and Sikic, 1999). Both PBOX-6 and nocodazole resulted in a dramatic destruction of the microtubule complex network of the cell, relative to the intricate mesh of microtubules witnessed in the vehicle control cells. The effect of PBOX-6 upon the microtubule network was distinct from that elicited by treatment with paclitaxel. Paclitaxel is a known microtubule polymerizer that, with increasing concentration, causes an increase in microtubule mass and a consequential distinctive "bundling" of the microtubules. It would therefore seem that PBOX-6 targets the microtubule network of the cell, causing its dissolution via microtubule depolymerization.

To address whether the differential response of the non- and proapoptotic subsets of PBOX compounds is based upon the ability to distort the microtubule network, the effect upon the microtubule network in MCF-7 cells of PBOX-15, another potent member of the proapoptotic subset of PBOX compounds, and PBOX-21, a member of the nonapoptotic PBOX compounds, was assessed. This revealed that PBOX-15 also disrupted the microtubule network of the cell in a manner similar to that of PBOX-6. In contrast, PBOX-21 had no effect upon the microtubule network of the cell, suggesting that the ability of a PBOX compound to inhibit microtubule polymerization determines its ability to induce apoptotic cell death.

The disassembly of the microtubule network after treatment with PBOX-6 and PBOX-15 suggested that they act as microtubule depolymerizing agents. To examine this hypothesis, the effect of PBOX-6 and PBOX-15 upon tubulin assembly in a cell-free system in vitro was assessed and compared with the effects of nocodazole and paclitaxel. The effect of PBOX-21 upon the assembly of tubulin in vitro was also determined as a negative control. These assays revealed that both PBOX-6 and PBOX-15 inhibit the assembly of tubulin in a dose-dependent manner, confirming them as microtubule depolymerizers. As expected, and in agreement with the literature, nocodazole inhibited tubulin assembly whereas paclitaxel induced tubulin assembly, both in a dose-dependent fashion. PBOX-21 had a negligible effect upon the assembly of tubulin relative to the vehicle control, suggesting once again that the differential response of members of the antiproliferative and proapoptotic subsets of PBOX compounds is linked to their ability to directly bind to and inhibit the polymerization of cellular microtubules.

It is notable that both 100 nM and 1 μM PBOX-6 were capable of inhibiting the assembly of tubulin in the cell-free assay system, whereas these concentrations were found to elicit no effect upon either the microtubule network of the cell or the cell cycle progression. This discrepancy between the concentrations of PBOX-6 that elicit an effect in a cell-free system and cell-based assay is possibly due to compound depletion and/or cell penetration effects. Discrepancies between the concentrations of antimicrotubule agents that elicit effects in cell-based and cell-free systems have been widely reported (Jiang et al., 1998a,b; Ling et al., 2002).

Although these PBOX compounds are less potent than some antimicrotubule agents such as paclitaxel, which inhibits cancerous cell growth at low nanomolar concentrations (IC_{50} value ~10 nM), some of these novel PBOX compounds, such as PBOX-15, are still effective in the nanomolar range (IC_{50} value ~250 nM). PBOX-15 is therefore much more potent than some other antimicrotubule agents, such as arsenic trioxide (Ling et al., 2002) and salvinal (Chang et al., 2004), which elicit effects in only the micromolar range (IC_{50} value ~10 μM for both compounds).

Antimicrotubule compounds can be classified into different categories depending on their binding sites on tubulin. Through the use of techniques such as photoaffinity labeling (Bai et al., 1996a,b; Rai and Wolff, 1996) and protein footprinting experiments (Chaudhuri et al., 2000), as well as the crystal structures identified by Downing and Nogales (1998), and more recently by Ravelli et al. (2004), specific binding residues and binding domains upon tubulin have been at least partially characterized for paclitaxel, vinblastine, and colchicine. *Vinca* alkaloids, rhizoxin, dolastetins, and spongistatin react with the domain for vinblastine. Colchicine, nocodazole, podophyllotoxin, and curacin A bind to the colchicine domain (Rai and Wolff, 1996). Because these are the only two defined binding sites of tubulin depolymerizers, it was necessary to determine whether PBOX-6 mediated its antimicrotubule activity via binding to either of these sites. The results from the competitive binding experiments revealed that PBOX-6 did not inhibit binding of either colchicine or vinblastine to tubulin, indicating that PBOX-6 has its

Downloaded from molpharm.aspetjournals.org at ASPET Journals on June 5, 2017

own, novel, binding site upon tubulin. Other antimicrotubule agents, such as estramustine (Panda et al., 1997), arsenic trioxide (Ling et al., 2002), naphthopyran (Dell, 1998), and cemadotin (Jordan et al., 1998), have also been shown to bind to as-yet-uncharacterized novel sites on tubulin.

In conclusion, we have identified tubulin as the molecular target of proapoptotic PBOX compounds such as PBOX-6. The clinical efficacy of antimicrotubule agents is well established, although increasing evidence of resistance to these agents has prompted the search for new agents with a similar mechanism. The ability of PBOX-6 to induce both cell death and cell cycle arrest, to bind tubulin, and to cause microtubule depolymerization identify it as a strong candidate for antineoplastic therapy.

References

Bai R, Pei XF, Boye O, Getahun Z, Grover S, Bekisz J, Nguyen NY, Brossi A, and Hamel E (1996a) Identification of cysteine 354 of β-tubulin as part of the binding site for the A ring of colchicine. *J Biol Chem* **271:**12639–12645.

Bai R, Schwartz RE, Kepler JA, Pettit GR, and Hamel E (1996b) Characterization of the interaction of cryptophycin 1 with tubulin: binding in the Vinca domain, competitive inhibition of dolastatin 10 binding and an unusual aggregation reaction. *Cancer Res* **56:**4398–4406.

Blagosklonny MV, Giannakakou P, el-Deiry WS, Kingston DG, Higgs PI, Neckers L, and Fojo T (1997) Raf-1/bcl-2 phosphorylation: a step from microtubule damage to cell death. *Cancer Res* **57:**130–135.

Brantley-Finley C, Lyle CS, Du L, Goodwin ME, Hall T, Szwedo D, Kaushal GP, and Chambers TC (2003) The JNK, ERK and p53 pathways play distinct roles in apoptosis mediated by the antitumor agents vinblastine, doxorubicin and etoposide. *Biochem Pharmacol* **66:**459–469.

Campiani G, Nacci V, Fiorini I, De Filippis MP, Garofalo A, Ciani SM, Greco G, Novellino E, Williams DC, Zisterer DM, et al. (1996) Synthesis, biological activity and SARs of pyrrolobenzoxazepine derivatives, a new class of specific "peripheral-type" benzodiazepine receptor ligands. *J Med Chem* **39:**3435–3450.

Chang JY, Chang CY, Kuo CC, Chen LT, Wein YS, and Kuo YH (2004) Salvinal, a novel microtubule inhibitor isolated from *Salvia miltiorrhizae* Bunge (Danshen), with antimitotic activity in multidrug-sensitive and -resistant human tumor cells. *Mol Pharmacol* **65:**77–84.

Chaudhuri AR, Seetharamalu P, Schwarz PM, Hausheer FH, and Luduena RF (2000) The interaction of the B-ring of colchicine with alpha-tubulin: a novel footprinting approach. *J Mol Biol* **303:**679–692.

Crespo NC, Ohkanda J, Yen TJ, Hamilton AD, and Sebti SM (2001) The farnesyltransferase inhibitor, FTI-2153, blocks bipolar spindle formation and chromosome alignment and causes prometaphase accumulation during mitosis of human lung cancer cells. *J Biol Chem* **276:**16161–16167.

Crown J and O'Leary M (2000) The taxanes: an update. *Lancet* **355:**1176–1178.

Dell CP (1998) Antiproliferative naphthopyrans: biological activity, mechanistic studies and therapeutic potential. *Curr Med Chem* **5:**179–194.

Donaldson KL, Goolsby GL, Kiener PA, and Wahl AF (1994) Activation of p34cdc2 coincident with Taxol-induced apoptosis. *Cell Growth Differ* **5:**1041–1050.

Downing KH and Nogales E (1998) New insights into microtubule structure and function from the atomic model of tubulin. *Eur Biophys J* **27:**431–436.

Dumontet C and Sikic BI (1999) Mechanisms of action of and resistance to antitubulin agents: microtubule dynamics, drug transport and cell death. *J Clin Oncol* **17:**1061–1070.

Friedman PA and Platzer EG (1978) Interaction of anthelmintic benzimidazoles and benzimidazole derivatives with bovine brain tubulin. *Biochim Biophys Acta* **544:**605–614.

Jiang JD, Davis AS, Middleton K, Ling YH, Perez-Soler R, Holland JF, and Bekesi JG (1998a) 3-(Iodoacetamido)-benzoylurea: a novel cancericidal tubulin ligand that inhibits microtubule polymerization, phosphorylates bcl-2 and induces apoptosis in tumor cells. *Cancer Res* **58:**5389–5395.

Jiang JD, Wang Y, Roboz J, Strauchen J, Holland JF, and Bekesi JG (1998b) Inhibition of microtubule assembly in tumor cells by 3-bromoacetylamino benzoylurea, a new cancericidal compound. *Cancer Res* **58:**2126–2133.

Jordan MA, Walker D, de Arruda M, Barlozzari T, and Panda D (1998) Suppression of microtubule dynamics by binding of cemadotin to tubulin: possible mechanism for its antitumor action. *Biochemistry* **37:**17571–17578.

Jordan MA and Wilson L (2004) Microtubules as a target for anticancer drugs. *Nat Rev Cancer* **4:**253–265.

King RW, Jackson PK, and Kirschner MW (1994) Mitosis in transition. *Cell* **79:**563–571.

Lee LF, Li G, Templeton DJ, and Ting JP (1998) Paclitaxel (Taxol)-induced gene expression and cell death are both mediated by the activation of c-Jun NH2-terminal kinase (JNK/SAPK). *J Biol Chem* **273:**28253–28260.

Ling YH, Jiang JD, Holland JF, and Perez-Soler R (2002) Arsenic trioxide produces polymerization of microtubules and mitotic arrest before apoptosis in human tumor cell lines. *Mol Pharmacol* **62:**529–538.

Mc Gee MM, Campiani G, Ramunno A, Nacci V, Lawler M, Williams DC, and Zisterer DM (2002a) Activation of the c-Jun N-terminal kinase (JNK) signaling pathway is essential during PBOX-6-induced apoptosis in chronic myelogenous leukemia (CML) cells. *J Biol Chem* **277:**18383–18389.

Mc Gee MM, Greene LM, Ledwidge S, Campiani G, Nacci V, Lawler M, Williams DC, and Zisterer DM (2004) Selective induction of apoptosis by the pyrrolo-1,5-benzoxazepine 7-[[dimethylcarbamoyl]oxy]-6-(2-naphthyl)pyrrolo-[2,1-*d*] (1,5)-benzoxazepine (PBOX-6) in Leukemia cells occurs via the c-Jun NH2-terminal kinase-dependent phosphorylation and inactivation of Bcl-2 and Bcl-XL *J Pharmacol Exp Ther* **310:**1084–1095.

Mc Gee MM, Hyland E, Campiani G, Ramunn A, Nacci V, and Zisterer DM (2002b) Caspase-3 is not essential for DNA fragmentation in MCF-7 cells during apoptosis induced by the pyrrolo-1,5-benzoxazepine, PBOX-6. *FEBS Lett* **515:**66–70.

Mulligan JM, Campiani G, Ramunno A, Nacci V, and Zisterer DM (2003) Inhibition of G_1 cyclin-dependent kinase activity during growth arrest of human astrocytoma cells by the pyrrolo-1,5-benzoxazepine, PBOX-21. *Biochim Biophys Acta* **1639:**43–52.

Nogales E, Wolf SG, and Downing KH (1998) Structure of the alpha beta tubulin dimer by electron crystallography. *Nature (Lond)* **391:**199–203.

Panda D, Miller HP, Islam K, and Wilson L (1997) Stabilization of microtubule dynamics by estramustine by binding to a novel site in tubulin: a possible mechanistic basis for its antitumor action. *Proc Natl Acad Sci USA* **94:**10560–10564.

Rai SS and Wolff J (1996) Localization of the vinblastine-binding site on β-tubulin. *J Biol Chem* **271:**14707–14711.

Ravelli RBG, Gigant B, Curmi PA, Jourdain I, Lachkar S, Sobel A, and Knossow M (2004) Insight into tubulin regulation from a complex with colchicine and a stathmin-like domain. *Nature (Lond)* **428:**(6979) 198–202.

Serrano L, Avila J, and Maccioni RB (1984) Limited proteolysis of tubulin and the localization of the binding site for colchicine. *J Biol Chem* **259:**6607–6611.

Shtil AA, Mandlekar S, Yu R, Walter RJ, Hagen K, Tan TH, Roninson IB, and Kong AN (1999) Differential regulation of mitogen-activated protein kinases by microtubule-binding agents in human breast cancer cells. *Oncogene* **18:**377–384.

Srivastava RK, Mi QS, Hardwick JM, and Longo DL (1999) Deletion of the loop region of Bcl-2 completely blocks paclitaxel-induced apoptosis. *Proc Natl Acad Sci USA* **96:**3775–3780.

Uppuluri S, Knipling L, Sackett DL, and Wolff J (1993) Localization of the colchicine-binding site of tubulin. *Proc Natl Acad Sci USA* **90:**11598–11602.

Wang TH, Popp DM, Wang HS, Saitoh M, Mural JG, Henley DC, Ichijo H, and Wimalasena J (1999) Microtubule dysfunction induced by paclitaxel initiates apoptosis through both c-Jun N-terminal kinase (JNK)-dependent and -independent pathways in ovarian cancer cells. *J Biol Chem* **274:**8208–8216.

Wang TH, Wang HS, Ichijo H, Giannakakou P, Foster JS, Fojo T, and Wimalasena J (1998) Microtubule-interfering agents activate c-Jun N-terminal kinase/stress-activated protein kinase through both Ras and apoptosis signal-regulating kinase pathways. *J Biol Chem* **273:**4928–4936.

Wassmann K and Benezra R (2001) Mitotic checkpoints: from yeast to cancer. *Curr Opin Genet Dev* **11:**83–90.

Woods CM, Zhu J, McQueney PA, Bollag D, and Lazarides E (1995) Taxol-induced mitotic block triggers rapid onset of a p53-independent apoptotic pathway. *Mol Med* **1:**506–526.

Zhou J, Gupta K, Yao J, Ye K, Panda D, Giannakakou P, and Joshi HC (2002) Paclitaxel-resistant human ovarian cancer cells undergo c-Jun NH2-terminal kinase-mediated apoptosis in response to noscapine. *J Biol Chem* **277:**39777–39785.

Zisterer DM, Campiani G, Nacci V, and Williams DC (2000) Pyrrolo-1,5-benzoxazepines induce apoptosis in HL-60, Jurkat and Hut-78 cells: a new class of apoptotic agents. *J Pharmacol Exp Ther* **293:**48–59.

Address correspondence to: Dr. Daniela Zisterer, School of Biochemistry and Immunology, Trinity College, Dublin 2, Ireland. E-mail: dzistrer@tcd.ie

Downloaded from molpharm.aspetjournals.org at ASPET Journals on June 5, 2017